REPORT DOCUMENTATION PAGE

Form Approved
OMB No 0704 0188

AD-A261 521

2. REPORT DATE	3 REPORT TYPE AND DATES COVERED
2/15/93	Interim June 1, 1990 to February 1993

4. TITLE AND SUBTITLE
The Thermal and Photochemical Disproportionation of the Oxo Bridged Dimer$[\{W^{V}\eta^{5}\text{-}C_5H_5)_2(CH_3)\}_2(\mu\text{-}O)][PF_6]_2$

5. FUNDING NUMBERS
C: N00014-90-J-1762
R and T Code: 4135025

6. AUTHOR(S)
Robert L. Thompson, Samkeun Lee, Michael D. Hopkins and N. John Cooper

7. PERFORMING ORGANIZATION NAME(S) AND ADDRESS(ES)
Department of Chemistry
University of Pittsburgh
Pittsburgh, PA 15260

8. PERFORMING ORGANIZATION REPORT NUMBER
--

9. SPONSORING/MONITORING AGENCY NAME(S) AND ADDRESS(ES)
Department of the Navy
Office of the Chief of Naval Research
Arlington, VA 22217-5000

10. SPONSORING/MONITORING AGENCY REPORT NUMBER

11. SUPPLEMENTARY NOTES
Submitted for publication in Organometallics

12a. DISTRIBUTION/AVAILABILITY STATEMENT
This document has been approved for public release and sale; its distribution is unlimited.

12b. DISTRIBUTION CODE
--

13. ABSTRACT *(Maximum 200 words)*

See attached

93-03720
25pg

14. SUBJECT TERMS
Oxo-Bridged/Disproportionation/Transition Metal/ Photochemistry/Optical Memory

15. NUMBER OF PAGES
22

16. PRICE CODE
--

17. SECURITY CLASSIFICATION OF REPORT	18. SECURITY CLASSIFICATION OF THIS PAGE	19. SECURITY CLASSIFICATION OF ABSTRACT	20. LIMITATION OF ABSTRACT
Unclassified	Unclassified	Unclassified	--

OFFICE OF NAVAL RESEARCH

Grant N00014-90-J-1762

R&T Code 4135025

TECHNICAL REPORT NO. 5

The Thermal and Photochemical Disproportionation of the Oxo-Bridged Dimer $[\{W^{V}(\eta^{5}\text{-}C_5H_5)_2(CH_3)\}_2(\mu\text{-}O)][PF_6]_2$

by

Robert L. Thompson, Samkeun Lee, Michael D. Hopkins, and N. John Cooper

Submitted for publication in Organometallics

Department of Chemistry
University of Pittsburgh
Pittsburgh, PA 15260

The Thermal and Photochemical Disproportionation of the Oxo-Bridged Dimer $[\{W^{V}(\eta^{5}\text{-}C_5H_5)_2(CH_3)\}_2(\mu\text{-}O)][PF_6]_2$

Robert L. Thompson, Samkeun Lee, Michael D. Hopkins, and N. John Cooper*

Department of Chemistry and

Materials Research Center

University of Pittsburgh

Pittsburgh, Pennsylvania 15260

Submitted to Organometallics

Abstract

The diamagnetic d^1-d^1 oxo-bridged dimer $[\{W^V(\eta^5\text{-}C_5H_5)_2(CH_3)\}_2(\mu\text{-}O)]^{2+}$ ($\mathbf{1}^{2+}$) undergoes a thermal disproportionation reaction in CD_3CN to give the d^0 monomer $[W^{VI}(\eta^5\text{-}C_5H_5)_2(O)(CH_3)]^+$ ($\mathbf{4}^+$) and the acetonitrile-trapped d^2 monomer $[W^{IV}(\eta^5\text{-}C_5H_5)_2(CH_3)(NCCD_3)]^+$ ($\mathbf{5}^+$-d^3). The reaction is first order in $\mathbf{1}^{2+}$, and ^1H NMR kinetic studies between 54°C and 72°C have established that there is a large enthalpic barrier to disproportionation with $\Delta H^{\ddagger} = 33.7 \pm 1.7$ kcal·mole^{-1} and a significant positive entropy of activation for this dissociative process ($\Delta S^{\ddagger} = 25.1 \pm 5.2$ cal K^{-1}·mole^{-1}), corresponding to $\Delta G^{\ddagger} = 26.23$ kcal·mole^{-1} at 25°C. The dimer $\mathbf{1}^{2+}$ is also subject to photodisproportionation, and the barrier to thermal disproportionation of $\mathbf{1}^{2+}$ is sufficiently large to allow determination of the quantum yield for photodisproportionation of $\mathbf{1}^{2+}$ to $\mathbf{4}^+$ and $\mathbf{5}^+$ in CH_3CN. The reaction was readily monitored by electronic spectroscopy, since the only visible absorptions in electronic spectra of $\mathbf{4}^+$ and $\mathbf{5}^+$ are the tails of UV absorptions at 330 nm ($\varepsilon = 525$ L mole^{-1} cm^{-1}) and 400 nm ($\varepsilon = 398$ L mole^{-1} cm^{-1}), respectively, while $\mathbf{1}^{2+}$ has a strong absorption at 525 nm ($\varepsilon = 23{,}600$ L mole^{-1} cm^{-1}) in the region characteristic of d^1-d^1 dimers spin paired by a linear oxo bridge. Quantum yield determinations established that $\mathbf{1}^{2+}$ photodisproportionates when irradiated in the UV ($\Phi_{310} = 0.081$) and when irradiated into the principal visible absorption ($\Phi_{530} = 0.014$).

Introduction

We recently reported that ferrocenium oxidation of $[W^{IV}(\eta^5\text{-}C_5H_5)_2(CH_3)(OCH_3)]$ in methylethylketone (MEK) led to formation of a W(V) dimer $[\{W^{V}(\eta^5\text{-}C_5H_5)_2(CH_3)\}_2(\mu\text{-}O)][PF_6]_2$, (**1**$[PF_6]_2$), established crystallographically to have a linear oxo bridge between the two metal centers.[1] This material is diamagnetic both in solution and in the solid state, despite the formal d^1-d^1 electron count, and this can be attributed to π-interactions between the frontier orbitals of the metal centers and a filled p-orbital of the bridging oxygen atom.[2,3]

The best known class of molecules in which a linear oxo bridge spin pairs two d^1 centers are the Mo(V) oxo complexes in which a $[Mo^{V}_2O_3]^{4+}$ core,[3] containing two mutually syn or anti terminal oxo ligands perpendicular to the Mo-O-Mo axis, is complexed by four bis-chelate dithiocarboxylate-type ligands such as an xanthate ($[S_2COR]^-$),[4,5] dithiocarbamate ($[S_2CNR_2]^-$),[5,6] or dithiophosphate ($[S_2P(OR)_2]^-$) ligand.[7,8] It is well established that many of these $[Mo^{V}_2O_3(S_2EX_n)_4]$ complexes are in thermal equilibrium with their Mo(IV) and Mo(VI) disproportionation products $[Mo^{IV}O(S_2EX_n)_2]$ and $[Mo^{VI}O_2(S_2EX_n)_2]$,[9-11] and we recently reported that in the dithiocarbamate system such equilibria can be photo-driven to give rise to marked photochromic behavior, as established in the specific cases of $[Mo^{V}_2O_3\{S_2CN(CH_2Ph)_2\}_4]$ (**2**) and the isologous complex $[W^{V}_2O_3\{S_2CN(CH_2Ph)_2\}_4]$ (**3**).[12] We suggested that this new class of photochromic transition metal complexes might find useful technical applications in the areas of optical memory systems and photoresists,[13] but determining the quantitative characteristics of the photochromic behavior was difficult in the dithiocarbamate systems because of the rapidity of the thermal recombination reactions.

Our initial synthetic reactions readily established that $\mathbf{1}^{2+}$, like **2** and **3**, undergoes facile photodisproportionation.[1] In the presence of CD_3CN as a trapping agent this results (Scheme I) in clean photolysis to give $[W^{VI}(\eta^5\text{-}C_5H_5)_2(O)(CH_3)]^+$ ($\mathbf{4}^+$) and $[W^{IV}(\eta^5\text{-}C_5H_5)_2(CH_3)(NCCD_3)]^+$ ($\mathbf{5}^+$-d^3), but, in sharp contrast with the cases of **2** and **3**, this

occurs under conditions under which thermal disproportionation is slow. This meant that $\mathbf{1}^{2+}$ provided the first case in which it was feasible to study independently the photochemical and thermal disproportionation of a d^1-d^1 dimer with a linear oxo bridge, and we now wish to report quantum yields for the photodisproportionation of $\mathbf{1}^{2+}$ in CH_3CN and kinetic parameters for the thermal disproportionation of $\mathbf{1}^{2+}$ in CD_3CN.

Experimental Section

General Procedures. All manipulations were carried out under a dry, oxygen-free nitrogen atmosphere by means of drybox or standard Schlenk techniques. Acetonitrile (CH_3CN) was distilled from CaH_2 before use. Deuterated acetonitrile (CD_3CN, 99.5% D, Aldrich), and deuterated nitromethane (CD_3NO_2, 99% D, 1% v/v TMS, Aldrich) were degassed by dry nitrogen purge before use. Ethylene glycol was used as received from Aldrich Chemical Co. Electronic spectra were recorded on an IBM 9430 UV-VIS spectrometer, fitted with thermostatted cell holders, while the solution temperature within the cells was kept constant by means of a circulating bath of 50% aqueous ethylene glycol. ^1H NMR spectra were recorded on a Bruker AF 300 spectrometer at 300 MHz; spectra were recorded using the solvent signal as an internal standard. Photolyses were performed using an Oriel 200 Watt mercury-xenon arclamp as a light source and Oriel interference filters were used as monochromators.

The compounds $[\{W^V(\eta^5\text{-}C_5H_5)_2(CH_3)\}_2(\mu\text{-}O)][PF_6]_2$, ($\mathbf{1}[PF_6]_2$), $[W^{VI}(\eta^5\text{-}C_5H_5)_2(O)(CH_3)]PF_6$, ($\mathbf{4}PF_6$), and $[W^{IV}(\eta^5\text{-}C_5H_5)_2(CH_3)(NCCH_3)]PF_6$, ($\mathbf{5}PF_6$), were all prepared according to previously published methods.[1]

Variable Temperature ^1H NMR Studies. ^1H NMR spectra were recorded on a Bruker AF 300 spectrometer at 300 MHz. Temperatures within the NMR probe were controlled by a Bruker variable temperature unit, which was calibrated against boiling and freezing distilled H_2O, and were monitored before and after each trial by monitoring the

chemical shifts of ethylene glycol resonances. A typical trial involved the loading of a sample of $\mathbf{1}[PF_6]_2$ (ca 5 mg, 0.005 mmol) and 0.5 mL of CD_3CN into an NMR tube in a darkened room. The tube was maintained at -78°C in the dark until the NMR probe had been brought to temperature. Just prior to loading into the probe, the sample tube was shaken several times to effect dissolution of $\mathbf{1}[PF_6]_2$.

The rate of thermal disproportionation of $\mathbf{1}^{2+}$ in CD_3CN was measured by quantitatively monitoring the disappearance of the cyclopentadienyl resonance of $\mathbf{1}^{2+}$ via integration. To obtain quantitative information from the NMR spectra, the long proton translational relaxation time (T_1) of the cyclopentadienyl protons in $\mathbf{1}^{2+}$ (T_1 = 2.13 s - T_1 values were measured by the inversion-recovery method and analyzed by Bruker AF300 software) required that a long pulse delay be employed to ensure full relaxation between pulses; for this reason a pulse delay of > $5T_1$ was used. Five sequential summed FID's were used to generate the spectrum for each point in the kinetic analysis; the time at which the third FID was accumulated was taken to be the time at which the observed spectrum had been recorded. This process allowed approximately 10 - 30 time points to be collected during the 1 - 5 h experiment duration at each temperature.

The first-order rate constants (k_1) for the thermal disproportionation of $\mathbf{1}^{2+}$ in CD_3CN were obtained from the slopes of plots of $\ln([\mathbf{1}^{2+}]_0/[\mathbf{1}^{2+}]_t)$ versus time (t) at nine different temperatures. The $\ln([\mathbf{1}^{2+}]_0/[\mathbf{1}^{2+}]_t)$ versus t plots were all linear for at least 3 half-lives. The free energies of activation ($\Delta G^{\ddagger}$) for the disproportionation at each temperature were then calculated from the k_1 values by means of the Eyring equation,[14] taking the transmission coefficient $\kappa = 1$ as is usual in dynamic NMR studies.[15] The activation enthalpies and entropies ($\Delta H^{\ddagger}$ and $\Delta S^{\ddagger}$) were calculated from the intercept and slope of plots of $\Delta G^{\ddagger}$ versus temperature (T).

The reported errors in k_1 and temperature represent one standard deviation from the least-squares fit of the experimental data, whereas the uncertainties in $\Delta G^{\ddagger}$ were calculated

according to the equation derived by Binsch.[16] Uncertainties in $\Delta H^{\ddagger}$ and $\Delta S^{\ddagger}$ were estimated from extreme least-squares fits for $\Delta G^{\ddagger}$ versus T plots.

Quantum Yield Determinations. Quantum yields were determined in a manner similar to that reported by Wegner and Adamson for the measurement of the photoaquation of Reinecke's salt.[17] An air cooled 200 Watt Oriel mercury-xenon arclamp was used as the light source and the light was collimated to give a beam of about 1 cm^2 in area which was passed through a water filter and a variable iris before monochromatization by appropriate interference filters (Oriel; 310 and 530 nm). The collimated, monochromatic light beam was passed through sample cells in a brass thermostated cell holder, the temperature of which was controlled to ± 0.2°C using a circulating bath of 50% ethylene glycol/H_2O. The temperature within the cell holder was monitored by a Fluke K-type thermocouple. Absorbances of irradiated samples were measured by rapidly transferring the cells to an IBM 9430 spectrometer fitted with a second thermostatted cell holder, which was connected to the same circulating bath as the irradiation cell holder through glass T-joints and insulated rubber tubing. The lamp output was determined immediately before each quantum yield measurement by means of an Aberchrome 540 chemical actinometer. This consisted of a toluene solution of the heterocyclic fulgide, (E)-α-(2,5-dimethyl-3-furyl-ethylidene)(isopropylidene)succinic anhydride[18] of known concentration and volume sealed inside a 1 cm quartz cell under vacuum. Aberchrome 540 undergoes a highly reversible conrotatory ring-closure reaction to give deep red 7,7a-dihydro-2,4,7,7,7a-pentamethylbenzo[*b*]furan-5,6-dicarboxylic anhydride, and the known quantum yields for the forward and reverse reactions were used to measure intensities in the 310-370 nm and 436-545 nm ranges respectively from plots of the absorbance increase or decrease at 494 nm versus time and application of the relation: $I = (V/\Phi_A\ \varepsilon_A\ l)(\Delta A/t)$ where I is the intensity in einstein sec^{-1}, V is the solution volume (3.00×10^{-3} L), Φ_A is the forward or reverse quantum yield for Aberchrome 540 photolysis (0.20 and 0.06), ε_A is the extinction

coefficient for Aberchrome 540 at 494 nm (8,200 L mole^{-1} cm^{-1}), l is the cell length (1.00 cm), and $\Delta A/t$ is the slope from the absorbance versus time plot (sec^{-1}).[19]

After the lamp intensity measurement, sample solutions of known volume were allowed to equilibrate thermally in the dark for at least 10 min and were then irradiated for periods such that absorbance at 525 nm decayed no more than 10-15% from the absorbance at $t = t_0$. Concentrations of sample solutions were chosen such that the absorbance at the irradiation wavelength was > 1.7 absorbance units (> 98% incident intensity absorption) and that the absorbance at the measuring wavelength (525 nm) was no larger than 2.2 - 2.3 absorbance units to ensure readability. Quantum yields Φ were determined from the slope of plots of ΔA at 500 nm versus t by means of the same relationship as that above. Each quantum yield reported at a particular wavelength is the average of three values obtained in independent runs.

Results and Discussion

Thermal Disproportionation of $1[PF_6]_2$. The ^{1}H NMR spectrum of 1^{2+} in CD_3CN is straightforward, and contains a large singlet at δ 6.09 assigned to the cyclopentadienyl rings and a singlet at δ 0.88 (with 2.4 Hz ^{183}W satellites) assigned to the methyl group. The absence of other signals establishes that 1^{2+} is the only cyclopentadienyl-containing complex present in solution, and that 1^{2+} is therefore kinetically or thermodynamically stable with respect to disproportionation in CD_3CN at room temperature. At higher temperatures, however, new cyclopentadienyl signals appeared at δ 5.16 and 6.58 and new methyl signals appeared at δ 0.22 and 1.28 in the ^{1}H NMR spectrum of a sample of 1^{2+} in CD_3CN. The new cyclopentadienyl signals were of equal intensity and were located on either side of the original cyclopentadienyl signal of 1^{2+}, and the new methyl signals were similarly of equal intensity and on either side of the original methyl signal. Comparison of the new signals with those of authentic samples[1]

permitted unambiguous assignment to the expected disproportionation products $\mathbf{4}^{+}$ and $\mathbf{5}^{+}$, produced as per Scheme I.

We have determined the kinetics of the thermal disproportionation reaction by ^{1}H NMR spectroscopy at temperatures from 54°C to 72°C using solutions which were *ca* 3 mmol L^{-1} $\mathbf{1}^{2+}$ in CD_3CN (see Experimental Section for details of sample preparation and spectra acquisition). The reaction is remarkably clean and the disappearance of $\mathbf{1}^{2+}$ was followed by monitoring the change in the integration of the cyclopentadienyl signal of $\mathbf{1}^{2+}$ relative to the solvent signal. It was assumed that the integration is directly proportional to the concentration of $\mathbf{1}^{2+}$, ($[\mathbf{1}^{2+}]$). Data were plotted assuming first-order kinetics in $[\mathbf{1}^{2+}]$ (as confirmed by the linearity of the plots to three half-lives) and a representative plot of ln $([\mathbf{1}^{2+}]_0/[\mathbf{1}^{2+}]_t)$ vs. time is shown in Figure 1. The slopes of these plots were used to obtain the first-order rate constants, k_1, and, hence, the free energies of activation, $\Delta G^{\ddagger}$, as summarized in Table II.

The separation of $\Delta G^{\ddagger}$ into its enthalpic and entropic components allowed us to determine that there is a large enthalpic barrier to disproportionation of $\mathbf{1}^{2+}$ ($\Delta H^{\ddagger} = 33.7 \pm 1.7$ kcal $mole^{-1}$) but that formation of the transition state is entropically favored with a positive entropy of activation ($\Delta S^{\ddagger} = 25.1 \pm 5.2$ cal K^{-1} $mole^{-1}$). This value is reasonable for a dissociative reaction, although the significance of the value is limited by the uncertainty in its determination (this uncertainty largely reflects the narrow temperature range over which it was practical to collect kinetic data - the boiling point of CD_3CN provided an upper bound, while the sharp temperature dependence of the reaction meant that the time scale of kinetic runs exceeded the reasonably available blocks of NMR time before the temperature could be lowered further than 54°C). The large $\Delta H^{\ddagger}$ could reflect the enthalpic cost of marked charge transfer in the transition state for disproportionation.

It is appropriate to compare these data with the values reported by Tanaka et al. for the disproportionation of $[Mo^{V}_2O_3(S_2EX_n)_4]$ (S_2EX_n = S_2CNEt_2, $S_2P(OEt)_2$, S_2PPh_2) in 1,2-dichloroethane on the basis of concentration-jump kinetics experiments.[11] The $\Delta G^{\ddagger}$

values for $\mathbf{1}^{2+}$ are 7-8 kcal mole^{-1} larger than those for the molybdenum complexes, in reasonable agreement with the increased kinetic stability of $\mathbf{1}^{2+}$, but it is difficult to see why the molybdenum complexes should have negligible entropies of activation for dissociation as reported. If this is correct, it implies that $\Delta H^{\ddagger}$ values for the molybdenum systems are only half that which we have observed for $\mathbf{1}^{2+}$, and the molybdenum data can only be reconciled with that for $\mathbf{1}^{2+}$, and with the nature of the reaction, if the transition state for disproportionation of $[Mo^{V}_2O_3(S_2EX_n)_4]$ complexes is much earlier along the reaction coordinate than it is for $\mathbf{1}^{2+}$. This could be the case if disproportionation is essentially initiated by a charge transfer which dominates the transition state - reduced stability of the 4+ oxidation state in the 5d tungstenocene dimer could markedly increase the enthalpic cost of such a charge transfer. It should be noted, however, that this might be expected to be a general factor in the kinetics of disproportionation reactions of d^1-d^1 dimers with linear oxo bridges, and we have seen no qualitative evidence for significant differences between the photochromic behavior of $[Mo^{V}_2O_3\{S_2CN(CH_2Ph)_2\}_4]$ and of $[W^{V}_2O_3\{S_2CN(CH_2Ph)_2\}_4]$.[12]

Photodisproportionation of $\mathbf{1}[PF_6]_2$ in CH_3CN. We have previously reported that solutions of $\mathbf{1}[PF_6]_2$ in CD_3CN exhibit marked photosensitivity, decolorizing in bright sunlight to give a mixture of $[W^{VI}(\eta^5\text{-}C_5H_5)_2(O)(CH_3)]^+$ ($\mathbf{4}^+$) and the trapped W(IV) photodisproportionation product $[W^{IV}(\eta^5\text{-}C_5H_5)_2(CH_3)(NCCD_3)]^+$ ($\mathbf{5}^+$-d^3).[1] This reaction is remarkably clean (see Figure 2), and this, together with the anticipation on the basis of the thermal disproportionation studies that disproportionation is not kinetically accessible at room temperature ($t_{1/2}$ = 33 d at 25°C), suggested that photolysis of $\mathbf{1}^{2+}$ in acetonitrile would be suitable for quantum yield determinations. This was confirmed by a Beer's Law plot of the visible maximum in the electronic spectrum of $\mathbf{1}^{2+}$ in CH_3CN at 28°C, which was linear (R^2 = 1.00) from concentrations of 2.49 x 10^{-5} mol L^{-1} to 8.30 x

10^{-5} mole L^{-1} and allowed determination of the extinction coefficient at 525 nm as 23,600 L $mole^{-1}$ cm^{-1}.

The strong visible absorption of $\mathbf{1}^{2+}$ at 525 nm (see Figure 3 and Table III) offered an obvious approach to monitoring the photolysis using the decrease in absorbance at this wavelength, and inspection of the electronic spectra of the photolysis products $\mathbf{4}^{+}$ and $\mathbf{5}^{+}$ (Figure 4 and Table III) established that this would be straightforward experimentally since neither of the products have electronic absorptions in this region. Monitoring at 525 nm allowed determination of the quantum yields for photodisproportionation of $\mathbf{1}^{2+}$ in CH_3CN following irradiation at 310 nm and 530 nm as described in the Experimental Section and reported in Table IV.

The quantum yields for photodisproportionation of $\mathbf{1}^{2+}$ are moderate in both the UV and visible regions of the spectrum, but show marked wavelength dependence. The main visible absorption is photoactive, establishing that this energy is above the threshold for disproportionation, but $\Phi_{310} : \Phi_{530} = 6$, suggesting that the dissociative state is not the lowest photoexcited state but could be a derived state which can be more efficiently populated from higher excited states.[20] This argument is consistent with our observation that, although an intense visible absorption at *ca* 500 nm is an almost universal characteristic of d^1-d^1 dimers spin paired through a linear oxo bridge,[21] this absorption is photoactive with respect to disproportionation in some systems (such as $\mathbf{1}^{2+}$ and the dithiocarbamate complexes **2** and **3**) but is photoinactive in other systems (such as the dithiophosphate complexes $[Mo_2^{V}O_3\{S_2P(OR)_2\}_4]$ (R = Et, Ph, Me)).[8]

Since CH_3CN is such an effective trapping reagent, it was unclear how important a role the CH_3CN played in driving the photodisproportionation reaction. This was a particularly central point to address in light of Tyler's elegant demonstration that photodisproportionation of $[\{Mo(\eta^5\text{-}C_5H_5)(CO)_3\}_2]$ and related dimers involves initial homolysis followed by coordination of a donor ligand to form a 19-electron species from which the electron transfer step occurs.[22]

The range of potential alternative solvents was limited by the need for a highly polar solvent to dissolve dicationic $\mathbf{1}^{2+}$ but we were able to probe the importance of the solvent by photolyzing $\mathbf{1}[PF_6]_2$ in the less coordinating solvent, CH_3NO_2. This clearly established that the presence of CH_3CN was not necessary to photodissociate $\mathbf{1}^{2+}$, since solutions of $\mathbf{1}^{2+}$ in CH_3NO_2 did change from purple to yellow in color following photolysis. Monitoring of this reaction by ^1H NMR in CD_3NO_2 revealed, however, that the reaction had generated the pure W(VI) complex, $\mathbf{4}^+$; no signals could be observed from the W(IV) complex, $\mathbf{5}^+$. This suggests that photodisproportionation is occurring, but that the W(IV) complex $\mathbf{5}^+$ is sufficiently reactive to abstract an O atom from CD_3NO_2. We had, therefore, been unable to eliminate solvent effects from the photolysis reaction, although we had also established that the presence of a nitrile trapping reagent is not required.

These experiments leave the exact mechanism of the photodisproportionation step undetermined. Since the reduction does require a metal to metal charge transfer at some stage, however, it is tempting to speculate that this may involve an inorganic example of the Sudden Polarization Effect,[23] and experiments to test this hypothesis are underway in the laboratory.

Conclusions

The spin paired d^1-d^1 oxo bridged dimer $[\{W(\eta^5\text{-}C_5H_5)_2(CH_3)\}_2(\mu\text{-}O)]^{2+}$ ($\mathbf{1}^{2+}$) undergoes first-order thermal disproportionation at moderately elevated temperatures in CD_3CN to give the d^0 oxo complex $[W(\eta^5\text{-}C_5H_5)_2(O)(CH_3)]^+$ ($\mathbf{4}^+$) and the d^3-acetonitrile trapped d^2 complex $[W(\eta^5\text{-}C_5H_5)_2(CH_3)(NCCD_3)]^+$ ($\mathbf{5}^+$-d^3). The large enthalpy of activation and favorable entropy of activation are consistent with a dissociative transition state in which an enthalpically expensive charge transfer is well advanced. The resulting half-life of 33 d at 25°C is sufficient to allow independent study of the analogous photodisproportionation of $\mathbf{1}^{2+}$. This gives an equimolar mixture of $\mathbf{4}^+$ and $\mathbf{5}^+$, and the

modest quantum yield for irradiation in the visible region (Φ_{550} = 0.014) suggests that the lowest photoexcited state does not lead directly to disproportionation but that this occurs from a derived excited state which can be more efficiently accessed by UV irradiation (Φ_{310} = 0.081).

Acknowledgements

This work was supported in part by the Office of Naval Research. We wish to thank Dr. Cecilia Philbin for helpful advice and instruction concerning the quantum yield determinations and Professor Greg Geoffroy for the gift of a sample of Aberchrome 540.

References

(1) Jernakoff, P.; Hayes, G.; Lee, S.; Cooper, N. J. Organometallics submitted for publication.

(2) Dunitz, J. D.; Orgel, L. E. J. Chem. Soc. **1953**, 2594.

(3) Holm, R. H. Chem. Rev. **1987**, 87, 1401.

(4) Blake, A. B.; Cotton, F. A.; Wood, J. S. J. Am. Chem. Soc. **1964**, 86, 3024.

(5) Thompson, R. L.; Lee, S.; Geib, S. J.; Cooper, N. J. submitted to J. Am. Chem. Soc.

(6) (a) Ricard, L.; Estienne, J.; Karagiannidis, P.; Toledano, O.; Fischer, J.; Mitschler, A.; Weiss, R. J. Coord. Chem. **1974**, 3, 227. (b) Garner, C. D.; Howlader, N. C.; Mabbs, F. E.; McPhail, A. T.; Onan, K. D. J. Chem. Soc. Dalton Trans. **1979**, 962.

(7) (a) Knox, J. R.; Prout, C. K. Acta Crystallogr. B **1969**, B25, 2281. (b) Aliev, Z. G.; Atoumyan, L. O.; Tkachev, V. V. Zh. Strukt Khim. **1975**, 16, 694.

(8) Thompson, R. L.; Geib, S. J.; Cooper, N. J. Chem. Mater., submitted.

(9) Barral, R.; Bocard, C.; Sérée de Roch, I.; Sajus, L. Tetrahedron Lett. **1972**, 1693.

(10) Chen, G.J.J.; McDonald, J. W.; Newton, W. E. Inorg. Chem. **1976**, 15, 2612.

(11) (a) Matsuda, T.; Tanaka, K.; Tanaka, T. Inorg. Chem. **1979**, 18, 454. (b) Tanaka, T.; Tanaka, K.; Matsuda, T.; Hashi, K. in Molybdenum Chemistry of Biological Significance; Newton, W. E.; Otsuka, K., Eds., Plenum Press: New York, 1980, p. 361.

(12) Lee, S.; Staley, D. L.; Rheingold, A. L.; Cooper, N. J. Inorg. Chem. **1990**, 29, 4391.

(13) (a) Photochromism - Molecules and Systems; Durr, H.; Bouas-Laurent, H.; Eds.; Elsevier: Amsterdam, 1990. (b) Emmelius, M.; Pawlowski, G.; Vollman, H. W. Angew. Chem. Int. Ed. Engl. **1989** 28, 1445.

(14) Glasstone, S.; Laidler, K. J.; Eyring, H. The Theory of Rate Processes, McGraw Hill: New York, 1941; p. 195.

(15) Binsch, G. Topics Stereochem **1968**, 3, 97.

(16) Binsch, G. in Dynamic Nuclear Magnetic Resonance Spectroscopy, Jackman, L. M.; Cotton, F. A., Eds.; Academic Press: New York, 1975, Chap. 3, equation 111

(17) Wegner, E. E.; Adamson, A. W. J. Am. Chem. Soc. **1966**, 88, 394.

(18) Davey, P. J.; Heller, H. G.; Strydon, P. J.; Whittall, J. Chem. Soc. Perkin Trans. II, **1981**, 202.

(19) Heller, H. G.; Langan, J. R. J. Chem. Soc. Perkin Trans II, **1981**, 341.

(20) (a) Adamson, A. W.; Fleischauer, P. D. Concepts in Inorganic Photochemistry; Krieger: Malabar, FL, 1984. (b) Ferraudi, G. J. Elements of Inorganic Photochemistry; Wiley: New York, 1988.

(21) Craig, J. A.; Harlan, E. W.; Snyder, B. S.; Whitener, M. A.; Holm, R. H. Inorg. Chem. **1989**, 28, 2082.

(22) Tyler, D. R. Accts Chem. Res. **1991**, 24, 325.

(23) (a) Dauben, W. G.; Ritscher, J. S. J. Am. Chem. Soc. **1970**, 92, 2925. (b) Wulfman, C. E.; Kumei, S. E. Science **1971**, 172, 1061. (c) Salem, L. Accts Chem. Res. **1979**, 12, 87. (d) Michl, J.; Bonacic-Koutecky, V. Electronic Aspects of Organic Photochemistry; Wiley: New York, 1990.

Figure 1. Representative first-order kinetics plot for the thermal disproportionation of $[\{W^{V}(\eta^{5}\text{-}C_5H_5)_2(CH_3)\}_2(\mu\text{-}O)][PF_6]_2$ (**1**$[PF_6]_2$) in CD_3CN at 331.5 K.

Figure 2. ^1H NMR spectrum of a solution of $[\{W^{V}(\eta^{5}\text{-}C_5H_5)_2(CH_3)\}_2(\mu\text{-}O)][PF_6]_2$ (**1**$[PF_6]_2$) in CD_3CN: (a) before and (b) after photolysis.

Figure 3. Electronic spectrum of $[\{W^{V}(\eta^{5}\text{-}C_5H_5)_2(CH_3)\}_2(\mu\text{-}O)][PF_6]_2$ (**1**$[PF_6]_2$) in CH_3CN.

Figure 4. Electronic spectra in CH_3CN of: (a) $[W^{VI}(\eta^{5}\text{-}C_5H_5)_2(O)(CH_3)]PF_6$ (**4**PF_6); (b) $[W^{IV}(\eta^{5}\text{-}C_5H_5)_2(CH_3)(NCCH_3)]PF_6$ (**5**PF_6).

Table I. Summary of ^1H NMR Spectra for Complexes $\mathbf{1}^{2+}$, $\mathbf{4}^{+}$, and $\mathbf{5}^{+}$ in CD_3CN

Compound	Chemical Shift / δ
1$[PF_6]_2$ $[\{W(\eta^5\text{-}C_5H_5)_2(CH_3)\}_2(\mu\text{-}O)][PF_6]_2$	6.09 (s, 20 H, 4 C_5H_5), 0.88 (s, 6 H, 2 CH_3)
4PF_6 $[W(\eta^5\text{-}C_5H_5)_2(O)(CH_3)]PF_6$	6.58 (s, 10 H, 2 C_5H_5), 1.28 (s, 3 H, CH_3)
5PF_6 $[W(\eta^5\text{-}C_5H_5)_2(CH_3)(NCCD_3)]PF_6$	5.16 (s, 10 H, 2 C_5H_5), 0.22 (s, 3 H, CH_3)

Table II. First-order rate constants (k_1) and free energies of activation ($\Delta G^{\ddagger}$) for disproportionation of $[\{W^{V}(\eta^5\text{-}C_5H_5)_2(CH_3)\}_2(\mu\text{-}O)][PF_6]_2$ in CD_3CN at various temperatures (T).

T / K	$k_1 \times 10^5$ / s^{-1}	$\Delta G^{\ddagger}$ / kcal·mole^{-1}
327 ± 0.3	7.78 ± 0.35	25.4 ± 0.1
330 ± 0.3	8.47 ± 0.40	25.6 ± 0.1
332 ± 0.3	13.8 ± 6.2	25.4 ± 0.1
337 ± 0.3	31.2 ± 1.5	25.3 ± 0.1
338 ± 0.3	32.6 ± 1.6	25.3 ± 0.1
340 ± 0.3	43.1± 2.0	25.3 ± 0.1
342 ± 0.3	68.9 ± 3.6	25.1 ± 0.1
343 ± 0.3	79.3 ± 4.0	25.1 ± 0.1
345 ± 0.3	112 ± 6	25.0 ± 0.1

Table III. Electronic Spectral Bands of Complexes $\mathbf{1}^{2+}$, $\mathbf{4}^{+}$, and $\mathbf{5}^{+}$ in CH_3CN

Compound		Absorption maxima, $cm^{-1} \times 10^{-3}$ (log ε)
$\mathbf{1}[PF_6]_2$	$[\{W^{V}(\eta^5\text{-}C_5H_5)_2(CH_3)\}_2(\mu\text{-}O)][PF_6]_2$	19.0 (4.37), 25.4 (3.49), 32.3 (4.20), 37.9 (3.99)
$\mathbf{4}PF_6$	$[W^{VI}(\eta^5\text{-}C_5H_5)_2(O)(CH_3)]PF_6$	30.3 (2.72)
$\mathbf{5}PF_6$	$[W^{IV}(\eta^5\text{-}C_5H_5)_2(CH_3)(NCCH_3)]PF_6$	25.0 (2.60)

Table IV. Disappearance quantum yields for the 525 nm band of $[\{W^{V}(\eta^5\text{-}C_5H_5)_2(CH_3)\}_2(\mu\text{-}O)][PF_6]_2$ in CH_3CN at 28.0°C.

λ (nm)	conc. $\times 10^{4}$ (mole L^{-1})	intensity $\times 10^{9}$ (einstein sec^{-1})	$\Delta A/t \times 10^{4}$ (sec^{-1})	Quantum yield, Φ
310	1.47	3.59	22.5	0.080
			22.9	0.081
			23.4	0.083
				avg. 0.081
530	1.04	1.39	1.57	0.014
			1.60	0.015
			1.52	0.014
				avg. 0.014

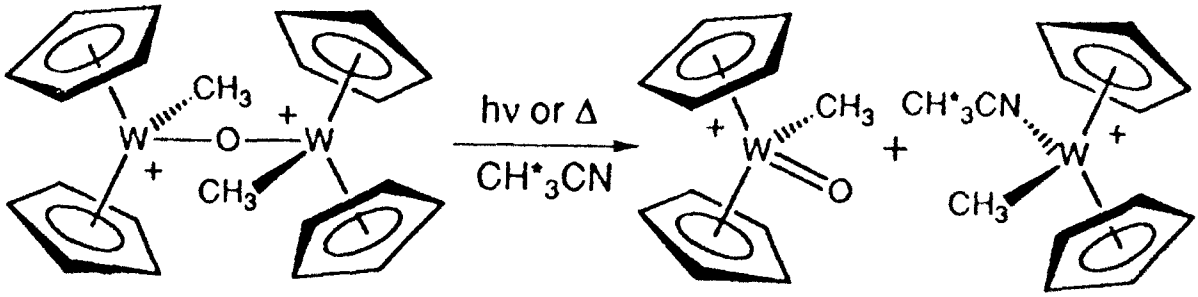

d^1 d^1 $\mathbf{1}^{2+}$ d^0 $\mathbf{4}^{+}$ d^2 $\mathbf{5}^{+}$

Scheme I

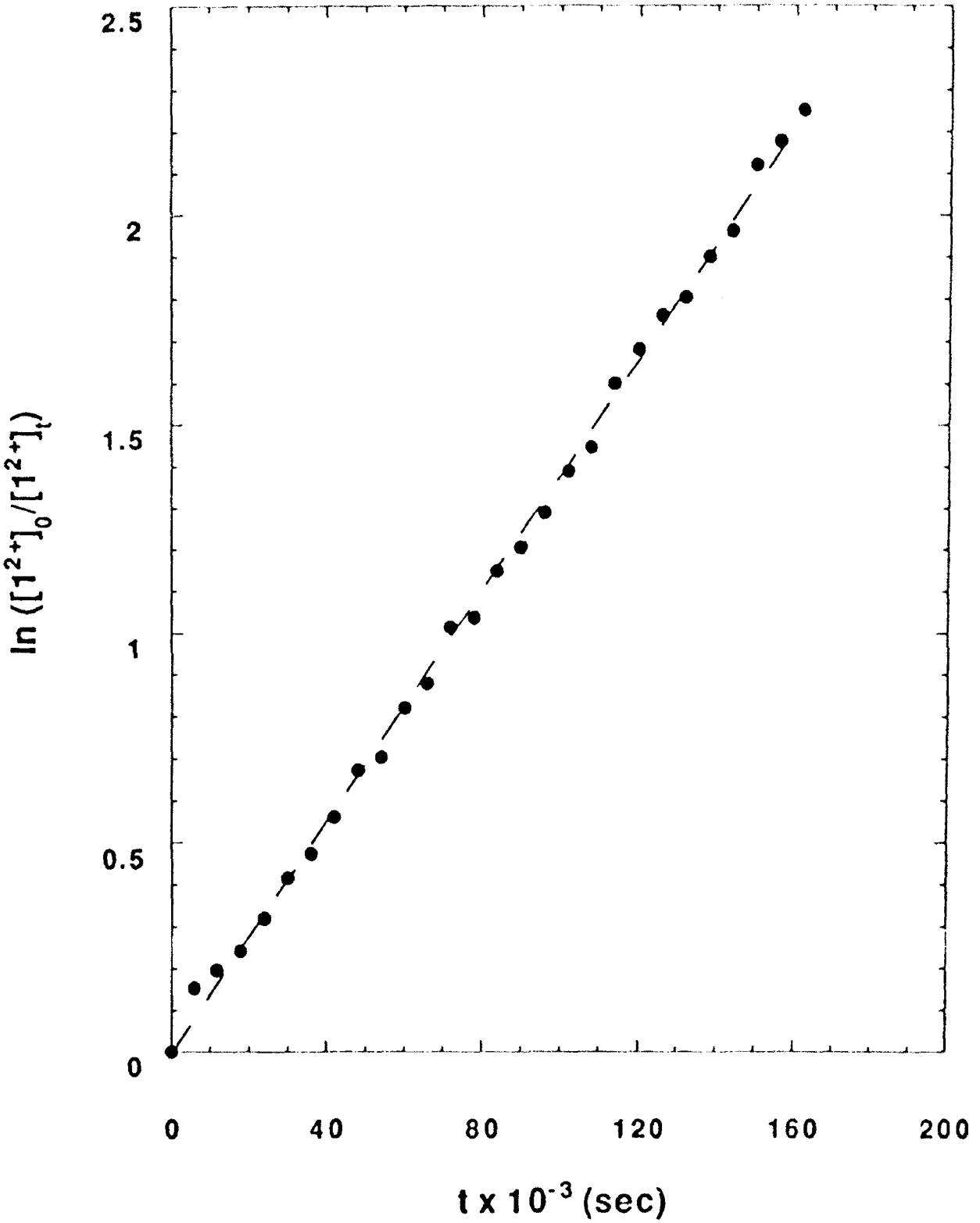
2.5
2
1.5
1
0.5
0
0
40
80
120
160
200
ln ([I2+]0/[I2+]t)
t x 10-3 (sec)

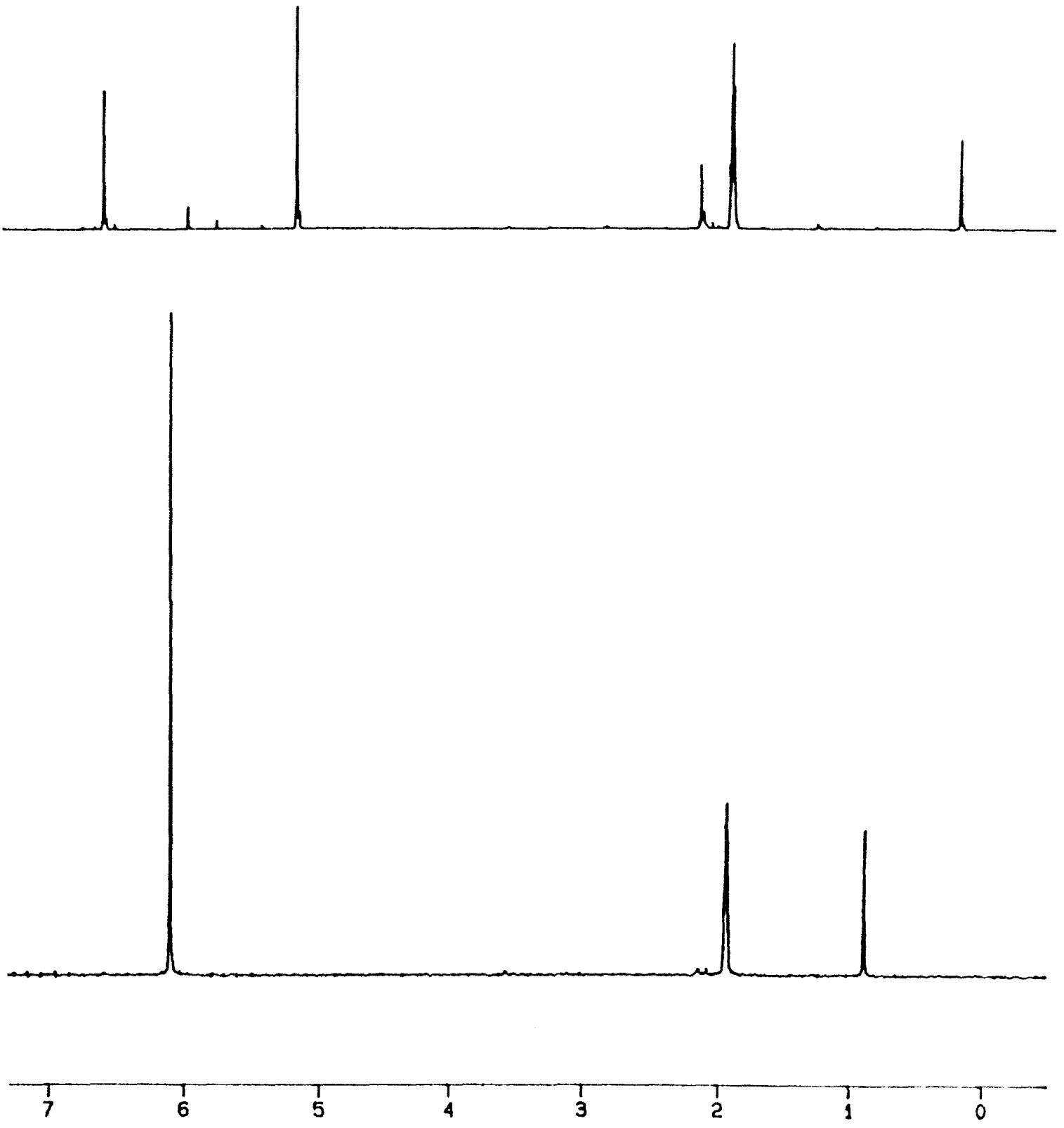
7
6
5
4
3
2
1
0

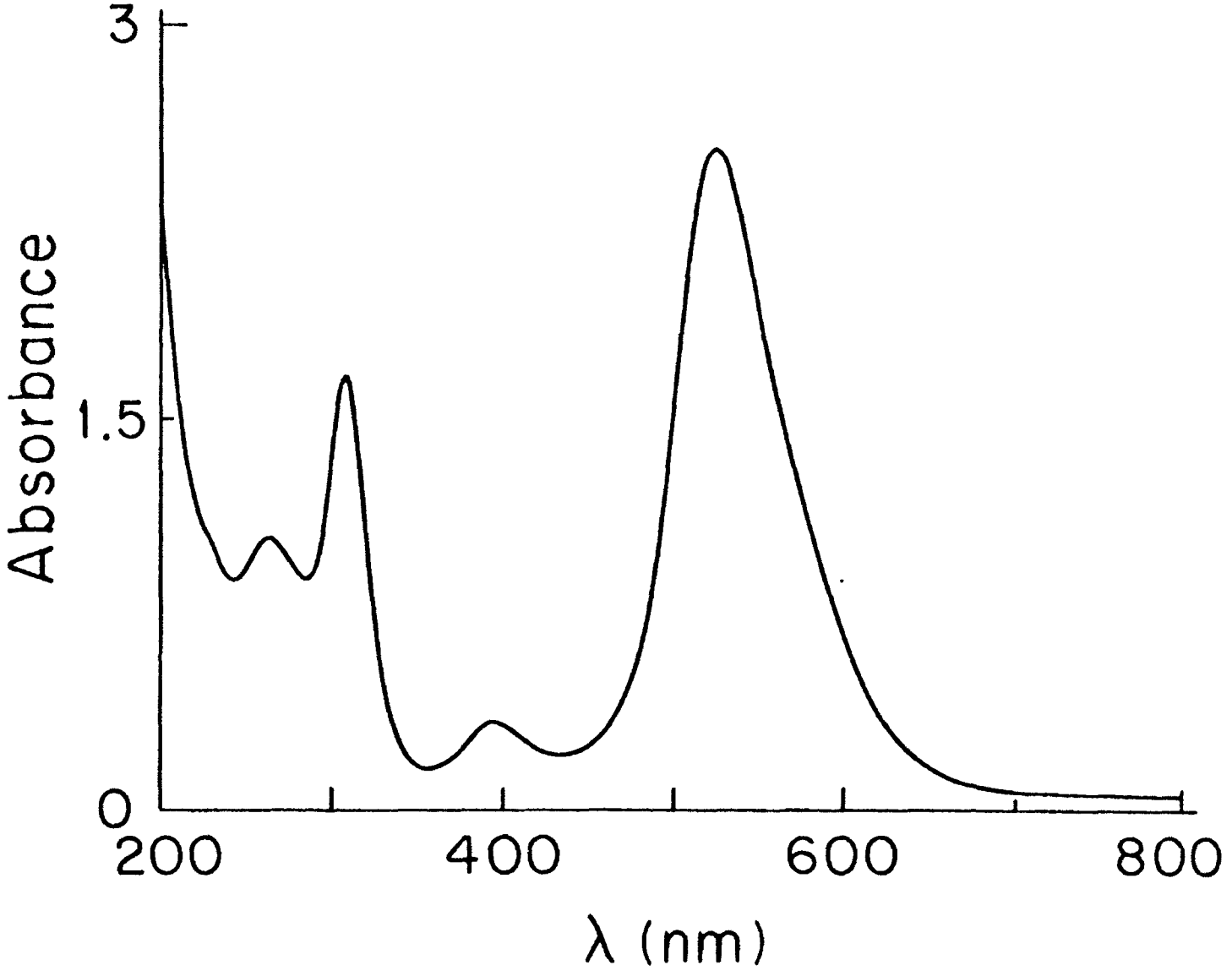
3
1.5
0
Absorbance
200
400
600
800
λ (nm)

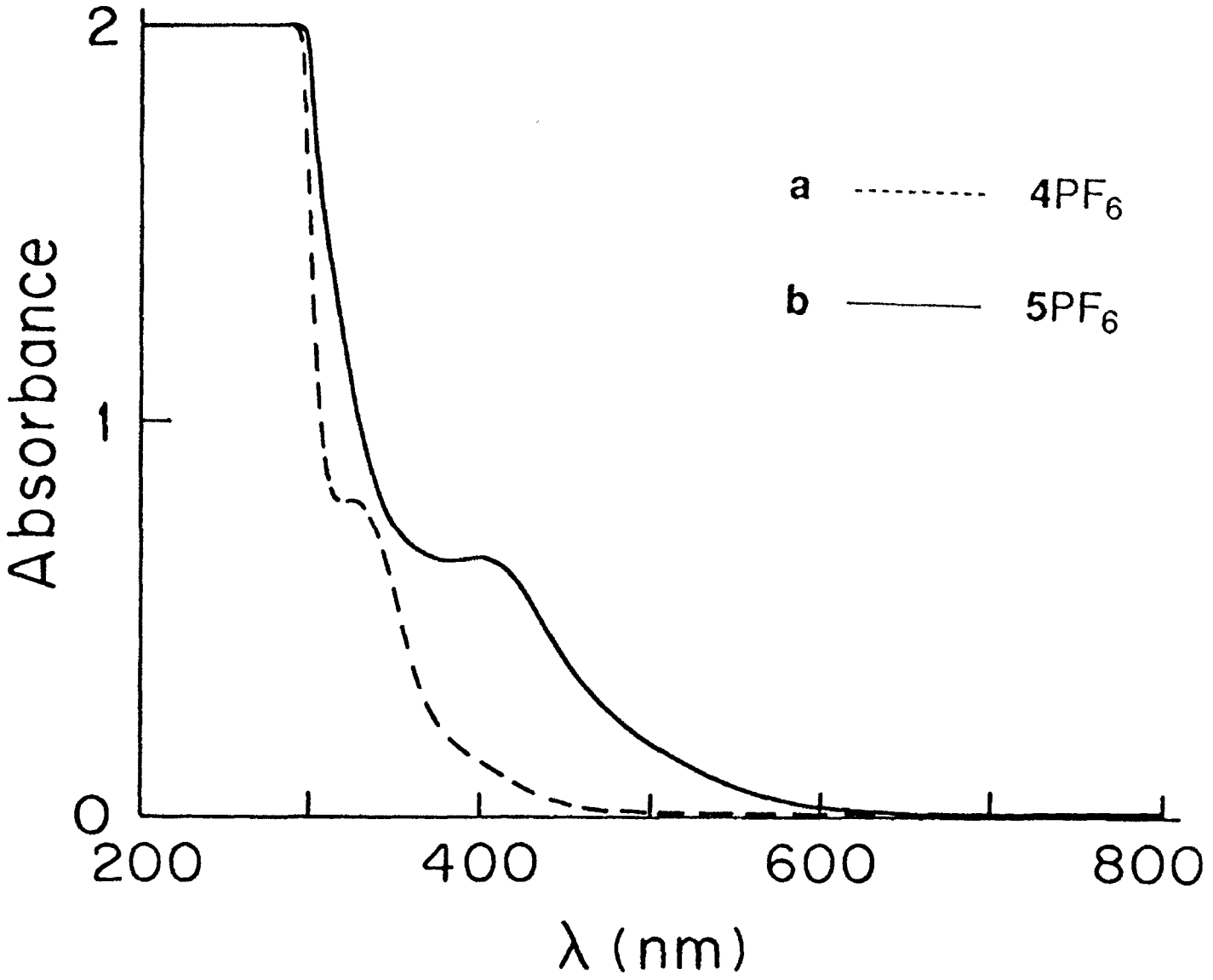
2
1
0
Absorbance
200
400
600
800
λ (nm)
a
4PF6
b
5PF6

TECHNICAL REPORT DISTRIBUTION LIST - GENERAL

Office of Naval Research (2)*
Chemistry Division, Code 1113
800 North Quincy Street
Arlington, Virginia 22217-5000

Dr. James S. Murday (1)
Chemistry Division, Code 6100
Naval Research Laboratory
Washington, D.C. 20375-5000

Dr. Robert Green, Director (1)
Chemistry Division, Code 385
Naval Air Weapons Center
Weapons Division
China Lake, CA 93555-6001

Dr. Elek Lindner (1)
Naval Command, Control and Ocean
Surveillance Center
RDT&E Division
San Diego, CA 92152-5000

Dr. Bernard E. Douda (1)
Crane Division
Naval Surface Warfare Center
Crane, Indiana 47522-5000

Dr. Richard W. Drisko (1)
Naval Civil Engineering
Laboratory
Code L52
Port Hueneme, CA 93043

Dr. Harold H. Singerman (1)
Naval Surface Warfare Center
Carderock Division Detachment
Annapolis, MD 21402-1198

Dr. Eugene C. Fischer (1)
Code 2840
Naval Surface Warfare Center
Carderock Division Detachment
Annapolis, MD 21402-1198

Defense Technical Information
Center (2)
Building 5, Cameron Station
Alexandria, VA 22314

* Number of copies to forward